Journal of Nuclear Medicine, published on October 23, 2020 as doi:10.2967/jnumed.118.213306

Imaging of the glucagon receptor in subjects with type 2 diabetes

Short title: Glucagon receptor PET in human

Authors: Olof Eriksson[1,2*], Irina Velikyan[3,4], Torsten Haack[5], Martin Bossart[5], Iina Laitinen[6], Philip J Larsen[5], Jan Erik Berglund[7], Gunnar Antoni[3,4], Lars Johansson[1], Stefan Pierrou[1], Joachim Tillner[8*], Michael Wagner[5*]

Affiliations:

1. Antaros Medical AB, Uppsala, Sweden
2. Science for Life Laboratory, Department of Medicinal Chemistry, Uppsala University, Uppsala, Sweden
3. Department of Medicinal Chemistry, Uppsala University, Uppsala, Sweden
4. Akademiska Sjukhuset, Uppsala, Sweden
5. R&D Research Platform, Integrated Drug Discovery, Sanofi, Frankfurt, Germany
6. Global Imaging, Sanofi, Frankfurt, Germany
7. Clinical Trial Consultants AB, Uppsala, Sweden
8. Translational Medicine, Sanofi, Frankfurt, Germany

*Corresponding authors:
Michael Wagner
Sanofi-Aventis Deutschland GmbH
Industriepark Hoechst, Building G838
D-65926 Frankfurt am Main, Germany
(c): +49 69 305 4875
(e): Michael.Wagner@sanofi.com

Joachim Tillner
Sanofi-Aventis Deutschland GmbH
Industriepark Höchst, Building H831

D-65926 Frankfurt am Main, Germany
(c): +49 69 305 6962
(e): joachim.tillner@sanofi.com

Olof Eriksson
Antaros Medical AB
Uppsala Science Park
Dag Hammarskjölds Väg 14B
SE-751 83 Uppsala, SWEDEN
(c): +46-707903054
(e): olof.eriksson@antarosmedical.com

Word count: 3319
Figures: 5
Tables: 1
ClinicalTrials.gov: NCT03350191

ABSTRACT

Rationale: Despite the importance of the Glucagon receptor (GCGR) in disease and in pharmaceutical drug development, there is a lack of specific and sensitive biomarkers of its activation in human. The Positron Emission Tomography (PET) radioligand ^{68}Ga-DO3A-VS-Tuna-2 (^{68}Ga-Tuna-2) was developed to yield a non-invasive imaging marker for GCGR target distribution and drug target engagement in humans.

Methods: The biodistribution and dosimetry of ^{68}Ga-Tuna-2 was assessed by PET/Computed Tomography (CT) in n=13 individuals with Type 2 Diabetes (T2D) as part of a clinical study assessing the occupancy of dual GCGR/Glucagon Like Peptide-1 Receptor (GLP-1R) agonist SAR425899. Binding of ^{68}Ga-Tuna-2 in liver and reference tissues was evaluated and correlated to biometrics (e.g. weight or BMI) or other biomarkers (e.g. plasma glucagon levels).

Results: ^{68}Ga-Tuna-2 binding was seen primarily in the liver, which is in line with the strong expression of GCGR on hepatocytes. Kidney demonstrated high excretion related retention, while all other tissue demonstrated rapid washout. The Standardized Uptake Value $(SUV)_{55min}$ uptake endpoint was sensitive to endogenous levels of glucagon. ^{68}Ga-Tuna-2 exhibited a safe dosimetry profile, and no adverse events after intravenous administration.

Conclusions: ^{68}Ga-Tuna-2 can be used for safe and accurate assessment of the GCGR in human. It may serve as an important tool in understanding the in vivo pharmacology of novel drugs engaging the GCGR.

Keywords: Glucagon, PET, metabolic disease, obesity, type 2 diabetes

INTRODUCTION

Glucagon is a crucial hormone in energy metabolism. It is secreted by the pancreatic alpha cells in response to decreased glucose availability in the blood stream. Glucagon exerts both autocrine (inhibition feedback), paracrine (on other islet cell subtypes including beta cells) and endocrine effects via activation of the glucagon receptor (GCGR). Its main endocrine action occurs in hepatocytes in the liver, where GCGR activation triggers breakdown of glycogen and subsequent release of glucose to the blood stream. Glucagon is a life-saving hormone to reverse hypoglycemia (*1*).

Glucagon signaling has furthermore been associated to increased energy expenditure. The GCGR has therefore recently come into focus also as a pharmaceutical target, especially in the context of bi- or trimodal peptide agonists for the treatment of metabolic disease and obesity (*2-4*). These usually combine GCGR agonism with agonism of one or both of the incretin hormone receptors; the Glucagon Like Peptide-1 Receptor (GLP1R) and the Gastric Inhibitory Peptide Receptor (GIPR).

Despite the importance of the GCGR in disease and in pharmaceutical drug development, there is a lack of specific and sensitive biomarkers of its activation in human physiology. Furthermore, some physiological effects of GCGR activation (inhibition of food intake, glucose homeostasis) tend to overlap with that of the incretins, making it difficult to disentangle GCGR target engagement and occupancy for the new class of poly-agonists. Based on this need, we recently developed the Positron Emission Tomography (PET) ligand ^{68}Ga-DO3A-VS-Tuna-2 (^{68}Ga-Tuna-2). ^{68}Ga-Tuna-2 (also known as ^{68}Ga-DO3A-GCG-S01) binds to the GCGR in liver with high specificity and affinity both in vitro and in vivo in several species including rat and non-human primate (*5-7*).

The dual GLP-1R/GCGR agonist SAR425899 demonstrated promising effects on weight loss and glucose control in preclinical and clinical studies (*8-11*). A clinical PET imaging study was therefore performed with the objective of evaluating the respective receptor occupancy of the dual agonist SAR425899 in individuals with Type 2 Diabetes (T2D) (ClinicalTrials.gov: NCT03350191). Occupancy of the GCGR in liver and GLP1R in pancreas was determined by baseline and on-drug PET/CT examinations using ^{68}Ga-

Tuna-2 and ^{68}Ga-DO3A-VS-Exendin4, respectively. The details of the clinical SAR425899 occupancy study was reported separately (*12*).

Here, we report the first-in-man results of the biodistribution, liver binding and dosimetry of ^{68}Ga-Tuna-2, based on the baseline examination of n=13 individuals with T2D.

MATERIALS AND METHODS

Study Population

The baseline ^{68}Ga-Tuna-2 examinations were performed as a part of a phase Ib, single center, open-label study assessing the GCGR and GLP1R occupancy of SAR425899 in overweight to obese T2D patients (ClinicalTrials.gov: NCT03350191). The results of the SAR425899 occupancy was reported separately (*12*). Individuals with a diagnosis of T2D for at least one year at the time of inclusion participated in the study (male or female, 18-75 years old). T2D related comorbidities were allowed. Otherwise, the individuals were generally healthy with normal vital signs as assessed by the investigator. Exclusion criteria included any medication except for stable metformin treatment, SU and medication for allowed comorbidities, pregnancy or breast-feeding. In total n=13 individuals with T2D underwent the ^{68}Ga-Tuna-2 baseline PET examinations, which are reported here. Body weight and fasting plasma glucose were measured at baseline and before breakfast and dosing at end-of-treatment. The study was approved by the Swedish Ethical Review Authority. All subjects signed a written informed consent. Study protocols were approved by the Swedish Medical Product Agency and the trial was performed in accordance with the guidelines established by the Declaration of Helsinki and the International Conference on Harmonization - Good Clinical Practice.

Radiochemistry

Good Manufacturing Practice grade DO3A-VS-Tuna-2 was provided by Sanofi. The Good Manufacturing Practice compliant production of ^{68}Ga-Tuna-2 was developed and conducted on an automated synthesizer (Modular Lab Pharm Tracer, Eckert & Ziegler, Germany) using disposable cassette system. The synthesis of ^{68}Ga-Tuna-2 for clinical studies was recently described in detail (*13*) and was developed based on, respectively a

manual radiolabeling procedure (*5*), as well as an automated procedure (*14*) developed earlier for similar peptide ^{68}Ga-DO3A-VS-Exendin4. The product formulated in saline containing ethanol (<10%) was supplied in a sterile glass vial. The radiochemical yield was over 90% with no unknown single impurity of over 5%.

PET/CT examination

Each individual was given standardized meals on the evening before, for breakfast, and lunch leading up to the PET scans to minimize variability in e.g. plasma glucagon levels. The lunch (lasagna) was administered 3h before the PET/CT examination, and the participants were otherwise fasting. Venous blood samples were collected just before the PET/CT examination for assessment of levels of endogenous glucagon. Blood was collected in P800 tubes™ (BD) to prevent proteolytic degradation and glucagon was analyzed using the Mercodia™ ELISA assay. Blood glucose was also assessed 5-, 30-and 60-minutes post-administration of PET radiopharmaceutical. The individuals were positioned with assistance of a CT scout (lateral, 120kV, 10 mAs) to include the liver in the 20cm Field of View of a Discovery MI PET/CT scanner (GE Healthcare, Milwaukee, MI, USA). Attenuation correction and anatomical co-registration was provided by a CT examination (120 kV, Auto mA 10-30 mA, noise-index 170, rotation-time 0.5s, full spiral, slice thickness 3.75 mm, pitch 1.53:1).

Then, a target dose of 0.5 MBq/kg ^{68}Ga-Tuna-2 was administered intravenously (0.46±0.031 MBq/kg, corresponding to 0.13±0.068 μg/kg DO3A-VS-Tuna-2 peptide mass). Dynamic PET measurements were acquired over 60 minutes and reconstructed by an iterative VPFX-S algorithm (3 iterations, 3 subsets, matrix 256x256, Z-axis post-filter 3mm) with all relevant corrections performed (30 frames in total; 12 x 10 s, 6 x 30 s, 5 x 120 s, 5 x 300 s, 2 x 600 s).

For three individuals, arterial sampling was performed 5, 30 and 60 min after ^{68}Ga-Tuna-2 administration to measure the radioactivity in whole blood and plasma (to calculate the plasma-to-whole blood concentration ratios) as well as to determine the metabolic stability of ^{68}Ga-Tuna-2 in humans.

Since this was a first-in-man study, each patient underwent additional monitoring before, during and after the administration of ^{68}Ga-Tuna-2 according to the local hospital

safety routines. The monitoring included inspection of injection site, and logging of blood pressure, 12-lead ECG, heart rate and general appearance throughout the imaging examination. A follow up ECG and inquiry on perceived adverse events is performed in person or over phone 24 h after the examination.

Metabolic stability

Blood samples were centrifuged at 4000 rpm for 2 minutes at 4°C (Beckman Allegra X-22R Centrifuge, Palo Alto, USA). From the plasma 0.5 ml was taken and an equal volume of acetonitrile was added to precipitate the proteins. The mixture was centrifuged at 13200 rpm at 4 °C for 1 min (Eppendorf 5415R centrifuge, Eppendorf AG, Hamburg, Germany). The supernatant was filtered through a 0.2µm nylon membrane (Corning Incorporated, Corning, NY, USA) by centrifugation at 13200 rpm at 4°C for 1 min. 500µl of the filtered supernatant was diluted with 1500µl H2O, and then 30µl 0.01mM of unlabeled DO3A-VS-Tuna-2 peptide was added to the mixture. The sample preparation recovery was determined by measuring the radioactivity in the plasma, filters and pellet.

High-Performance Liquid Chromatography analysis was performed using a binary pump system (Gilson, Middleton, USA). 1.8 ml of the sample was injected using an automated solid phase extraction controller (ASPEC Gilson) connected to a dilutor (Gilson). The separation was performed on a Xbridge Prep BEH130 C18 (peptide separation technology) 250mm x 10mm i.d 5µm with a 10x10 mm C18 security guard from the same supplier. The High-Performance Liquid Chromatography system was operated at a flow rate of 6 ml/min. The mobile phase consisted of 0.1% TFA in MilliQ: 0.1% TFA in Acetonitrile. Gradient elution mode was used for the separation (Gradient: 0-7 min: 5-70%, 7-12 min: 70%, 12-13 min: 70-5%, 13-15 min: 5%)

A second method was developed with a lesser gradient, to determine if any metabolites were co-eluting with the DO3A-VS-Tuna-2 peak. A UV detector (Gilson) was used to detect unlabeled DO3A-VS-Tuna-2 at 220nm. The outlet from the detector was connected to a switching valve on the arm of the ASPEC to enable automatic fraction collection. Six fractions were collected and the radioactivity in the fractions was measured

by a well-type scintillation counter. A radio detector (Radiomatic 610TR, Packard, USA) was coupled in series with the UV detector.

PET image analysis

Tissues of interest (liver, kidney, spleen and erector spinae muscle) were segmented on co-registered PET/CT images normalized to display the Standardized Uptake Value (SUV, i.e. corrected for administered dose in MBq and body weight) in each voxel (Carimas software v2.9, Turku PET Center, Turku, Finland). The full organ volume was segmented if inside the field of view. The liver segmentation was further divided into to the left and right part of the liver, approximately divided by a hypothetical diagonal line from the gallbladder to the vena cava (i.e. Cantlie's line). The aorta was delineated by segmenting single voxels fully within the lumen of aorta descendant as identified on early PET frames and co-registered CT projections.

Human predicted dosimetry

The dosimetry of ^{68}Ga-Tuna-2 was estimated based on the dynamic biodistribution in human abdomen. Briefly, the SUV values in each tissue at several time points (5, 10, 20, 30, 40, 50 and 60min) were normalized to that of a human adult whole body reference phantom (ICRP60). In tissues where human biodistribution was not available (due to the limited field of view of the scanner), data from non-human primate was imputed. The decay-corrected and normalized SUVs were back-corrected to count rates to calculate the actual radiation burden in each tissue. The tissue residence times (MBq*h/MBq) were assessed by trapezoidal approximation of the back-corrected biodistribution data. The residence time from the last measured time point (60 min) until infinity in each tissue was estimated as mono-exponential decay of the nuclide (assuming negligible washout).

The absorbed dose in an adult reference male phantom (ICRP60) was calculated from the residence time in each tissue (OLINDA/EXM 1.1 software, VanderBilt University, Nashville, USA). The organ specific doses are reported as mGy/ MBq (effective dose as mSv/MBq). The amount of MBq that can be safely administered annually (MBq/year) was calculated for each organ as well as the effective dose, by dividing the limiting dose (10 mSv/year for the effective dose, 150 mGy/year for all tissues

except for red marrow with 50 mGy/year) by the absorbed dose per MBq (mGy/MBq or mSv/MBq). Extrapolation of human dosimetry was previously performed based on rat *(5)* and non-human primate (*6*) biodistribution in a similar manner; these are here included for comparison.

Statistics

Data on group level are reported as means±SD. Statistical analysis was performed in GraphPad Prism 6.0, and differences between groups were assessed by the students *t*-test using a significance level of $p<0.05$.

RESULTS

Patient population

The age of the patient population (n=13) was 65.9±8.8 (range 49-75) years. The body weight was 97.77±8.09 (range 79-111) kg and the body mass index was 31.38±2.96 (range 27.76-37.20) kg/m^2. The majority was male (12 [92.3%] of 13 patients).

There occurred no adverse events during the ^{68}Ga-Tuna-2 PET scans and all n=13 baseline examination was performed in their entirety as planned.

The results of the occupancy of SAR425899 was reported separately (*12*). Briefly, SAR425899 demonstrated stronger activity on the GLP1R in pancreas (on average 48% occupancy) than on the GCGR in liver (on average 11% occupancy), which was in line with the in vitro potency on the respective receptor.

Biodistribution of ^{68}Ga-Tuna-2

On a group level ^{68}Ga-Tuna-2 rapidly accumulated in the blood pool (Figure 1A, top left panel and B), followed by extraction into liver and kidney and to a lesser extent tissues such as spleen (Figure 1A, top right panel). Uptake in spleen and blood pool was progressively cleared during the examination (Figure 1A, bottom left and right panels) while retention was seen in liver and kidney. The biodistribution on group levels is summarized in Figure 1B.

The dynamic analysis showed that the hepatic uptake displayed strong retention over 60 minutes in all individuals (Figure 2A). The spleen exhibited similar early tracer delivery as the liver, but then demonstrated rapid washout of tracer (Figure 2B). The aorta similarly displayed fast clearance in all individuals (Figure 2C). The SUV value during the last 10 minutes time frame, 50-60 minutes after administration (i.e. SUV_{55min}) provided the optimal image contrast for GCGR positive tissue liver compared to GCGR negative spleen and the aorta, and was therefore used as surrogate endpoint for GCGR density.

^{68}Ga-Tuna-2 uptake in liver was high (Liver SUV_{55min} = 3.96±0.80) at the end of the examination, indicating high density of glucagon receptors (Figure 2D). The amplitude of the hepatic binding was significant in comparison with GCGR negative spleen (Splenic

SUV_{55min} = 1.21±0.38, p<0.0001) and the aortic blood pool (Aortic SUV_{55min} = 1.40±0.42, p<0.0001). The spleen exhibited similar or lower uptake as the blood pool, indicating negligible binding of ^{68}Ga-Tuna-2.

Arterial blood samples were acquired after ^{68}Ga-Tuna-2 administration, for measurement of radioactivity in plasma and whole blood, as well as the metabolic stability of the radiolabeled peptide in plasma. The rate of metabolic degradation of ^{68}Ga-Tuna-2 in arterial plasma was relatively slow with approximately 85% intact tracer after 60 minutes (Table 1). The plasma-to-blood partition ratio was estimated to be constant throughout the examination (approximately 1.9).

GCGR density in different liver parts

There was a distinct difference in uptake of ^{68}Ga-Tuna-2 between the right and left parts of the liver, indicating a heterogeneous distribution of the GCGR in liver (Figure 3A-C). The binding in the left part was on average 20.5±8.7% (range 6.2-39.0) lower than in the right part. A decrease was seen in all individuals, but was also apparent on a group level. The difference was increasingly seen from 1 minutes and forward, but not during the initial biodistribution/ perfusion phase (<30s), where uptake in the left part in fact was higher (Figure 3D).

Sensitivity to levels of co-administered DO3A-VS-Tuna-2 peptide and endogenous glucagon

Liver uptake measured as SUV_{55min} at the baseline examination correlated to the levels of glucagon in plasma (R^2=0.33, p<0.05) (Figure 4A). This is expected to some degree, as ^{68}Ga-Tuna-2 engage the same binding site as endogenous glucagon. Thus, if the baseline value is to be compared to an assessment in which the subject exhibited lower or higher endogenous plasma glucagon levels, a correction should be performed.

There was no mass effect (i.e. significant blocking effect of the amount of unlabeled DO3A-VS-Tuna-2 peptide co-administered with the tracer dose) in liver uptake expressed as SUV_{55min} due to the peptide mass dosages given at the baseline examination

(Figure 4B). This is in line with the dose escalation data in non-human primate, where negligible mass effect was observed as peptide doses <0.2 µg/kg DO3A-VS-Tuna-2.

Correlations to physiological factors

GCGR density in liver did not correlate with factors such as weight (R^2=0.16, p=0.18), Body Mass Index (R^2=0.02, p=0.64) or age (R^2=0.12, p=0.25).
However, GCGR density correlated inversely with liver volume (R^2=0.55, p<0.01) (Figure 4C), i.e. in individuals with a large liver the density of GCGR is low.
Although anecdotal, the only female (1/13) enrolled in the study exhibited the higher GCGR density in liver (SUV_{55min}=5.4). The same individual additionally had among the lower GCGR heterogeneity between the right and left liver parts.

Human predicted dosimetry

Human predicted dosimetry of ^{68}Ga-Tuna-2 was based on human, NHP and rat biodistribution data (Figure 5A) and the regulatory acceptable amounts of MBq of ^{68}Ga-Tuna-2 that can be administered annually were based on the dosimetry calculations (Figure 5B). The limiting organ, based on human biodistribution data, is kidney, which still allows for 437 MBq per year. Thus, 4 PET examinations using up to 100 MBq ^{68}Ga-Tuna-2 are possible. ^{68}Ga-Tuna-2 thus has a safe dosimetry profile.

DISCUSSION

^{68}Ga-Tuna-2 displays the expected biodistribution of a small peptide labeled with Gallium-68, exhibiting fast clearance from most tissues in combination with strong excretion related retention in the kidney cortex. The strong retention in kidney (especially kidney cortex) is expected to be mainly due to urinary excretion and tubular reabsorption of the radiolabeled peptide. Kidney expression of GCGR has been reported (*15*), and part of the renal signal may originate from receptor-mediated binding, but is unlikely to be significant based on e.g. on the lack of blocking eefect seen in kidney in non-human primates (*6*). The uptake and retention in human liver, with high density of GCGR, was elevated, in line with preclinical data in rat and non-human primate.

SUV at the 55 minutes time point was selected as endpoint for assessing GCGR tissue density, as the liver-to-aorta was highest at this time-point. PET kinetic data can sometimes be analyzed by compartmental or graphical models in order to increase precision. Such analysis entails estimation of an input signal, usually from the arterial curve (corrected for metabolism and plasma-to-blood ratio). However, the liver is physiologically unique in this regard as it is supplied with both arterial and venous blood; arterial blood from the hepatic artery, as well as venous blood by the portal vein. The hepatic portal vein provides the main supply, approximately 70%, of blood to the liver. Thus, kinetic modeling of PET uptake is complicated because of the need for two distinct input signals. Furthermore, the ratio between the venous and arterial contribution is affected by arterial stiffening, a consequence of metabolic disease. Amelioration of vascular disease by therapeutic intervention in individuals with T2D can therefore likely change the venous/ arterial input signal in the liver. Because of the potential complexity in modeling the hepatic uptake, SUV was deemed as an acceptable endpoint.

The peptide mass dose of DO3A-VS-Tuna-2 in the study was estimated from dose escalation data in non-human primate. From the preclinical study, it was assessed that peptide doses below 0.2 μg/kg should elicit negligible mass effect (i.e. self-blocking on the glucagon receptor which could mask other interactions on the receptor). In the study, all

subject except one received the targeted dose <0.2 µg/kg. No appreciable mass effect was seen in the subject receiving just over 0.3 µg/kg either.

As demonstrated by the sensitivity of ^{68}Ga-Tuna-2 to endogenous glucagon levels, there is a possibility that changes to the endogenous levels of glucagon interfere with the calculation of GCGR density or occupancy. Thus, it is important to ensure fasting, or to administer a standardized meal before the examination, in addition to record the plasma glucagon levels for potential correction.

However, the conclusions drawn from the observed correlations (or their absence) are limited by the relatively small amount of examined subjects (n=13), where outliers can have large impact.

An interesting and consistent feature of ^{68}Ga-Tuna-2 was the clear difference in the right and left part of the liver. The left part exhibited on average 20% lower binding in all examined individuals. Importantly, there was no difference in right and left liver part uptake during the initial perfusion phase (0-1 min) indicating that the decreased retention of ^{68}Ga-Tuna-2 in the left part represents actual lower GCGR density rather than impaired regional hepatic perfusion or tracer delivery (Figure 3D). Furthermore, heterogeneous liver distribution of several established radiopharmaceuticals has previously been reported (*16*). Some exhibited up to 25% higher uptake in the left part (^{123}I-MIBG), a monoclonal antibody showed no difference between liver parts, and others demonstrated between 10-34% increased uptake in the right part. Since there is no consistent shift to either part reported, it implies that there is no general difference in perfusion at basal physiology. ^{68}Ga-Tuna-2 binding patterns consequently suggest an increased GCGR density in the right part of the liver.

GCGR density in liver as assessed by ^{68}Ga-Tuna-2 did not correlate with weight, BMI or age in this cohort of individuals with T2D. On the other hand, there was a negative correlation between GCGR density and liver volume (R^2=0.55, $p<0.01$), i.e. larger livers exhibited lower GCGR density (and consequently lower hepatocyte density). Liver

volume, especially in T2D, may be expanded by fat content due to Non-alcoholic Fatty Liver Disease (NAFLD) or Non-alcoholic SteatoHepatitis (NASH). Furthermore, high hepatic content of glycogen due to chronic increased B-glucose in turn tends bind water, thereby enlarging the liver. An enlarged liver with unchanged amount of hepatocytes will results in an apparent decrease in hepatocyte density (and subsequently GCGR density). The negative correlation for ^{68}Ga-Tuna-2 and liver volume likely reflect these two processes. Any dysregulation of GCGR expression in T2D compared to non-diabetic individuals is unknown but could potentially be explored with this novel technique.

Dynamic PET distribution scan of the entire body (several sequential whole body passes) would be ideal for dosimetry calculations. This was not performed as it was deemed to taxing on the enrolled individuals, as they already underwent 4 PET examinations in the full occupancy study. Thus, we only have access to the dynamic uptake in the abdominal region. However, as this region includes the critical tissues kidney, liver, red marrow and blood (as determined from rat and NHP distribution), we deem it suitable for dosimetry estimation (using NHP data imputation for missing, but not critical, tissues). The resulting dosimetry profile based on the human biodistribution is similar to that as predicted from non-human primate. This is further evidence that ^{68}Ga-Tuna-2 can be used for repeated PET/CT scanning annually, in combination with other radiopharmaceutical agents, from a radiation safety point of view.

In summary, ^{68}Ga-Tuna-2 biodistribution in human is consistent with the known distribution of GCGR. We foresee that ^{68}Ga-Tuna-2 can be used for assessment of liver target engagement and occupancy studies, for the emerging class of bi-or trimodal peptides targeting GCGR, in addition to e.g. GLP1R. Furthermore, this technique may improve the understanding on the role of GCGR in health in disease, e.g. by assessing its variability of receptor expression in T2D compared to non-diabetic subjects.
Furthermore, ^{68}Ga-Tuna-2 demonstrates a safe profile in regards to dosimetry and adverse events, when given intravenously at microdoses.

CONCLUSION

^{68}Ga-Tuna-2 can be used for safe and accurate assessment of the GCGR in human. It may serve as an important tool in understanding the in vivo pharmacology of novel drugs engaging the GCGR.

ACKNOWLEDGEMENTS

The study was sponsored in full by Sanofi. We thank Eduard Kober, Hélène Savoye (both employed by Sanofi), and Mélanie Bovo (employed by Business France) for their support during the conduct and analysis of this study.

AUTHOR CONTRIBUTIONS

O.E. researched data, designed the study and wrote the manuscript. I.V. researched data and reviewed the manuscript. T.H. researched data and reviewed the manuscript. M.B. researched data and reviewed the manuscript. I.L. contributed to data analysis and reviewed the manuscript. PJ.L. researched data and reviewed the manuscript, J.E.B. researched data and reviewed the manuscript. G.A. designed the study and reviewed the manuscript. L.J. designed the study and reviewed the manuscript. S.P. researched data and reviewed the manuscript. J.T. researched data, designed the study and reviewed the manuscript. M.W. designed the study and wrote the manuscript.

DISCLOSURES

Torsten Haack, Martin Bossart, Iina Laitinen, Philip J Larsen, Joachim Tillner, Michael Wagner are employees of Sanofi-Aventis. Olof Eriksson, Stefan Pierrou and Lars Johansson are employees of Antaros Medical AB. Jan Erik Berglund is an employee of CTC AB. No other potential conflicts of interest relevant to this article exist.

KEY POINTS

QUESTION: Despite the importance of the glucagon receptor in metabolic disease and in pharmaceutical drug development, there is a lack of specific and sensitive biomarkers of its activation in human.

PERTINENT FINDINGS: In vivo imaging of hepatic glucagon receptors was feasible by ^{68}Ga-Tuna-2 PET/CT. ^{68}Ga-Tuna-2 was sensitive to endogenous levels of glucagon,

exhibited a safe dosimetry profile combined with no adverse events after intravenous administration.

IMPLICATIONS FOR PATIENT CARE: ^{68}Ga-Tuna-2 can be used for safe and accurate imaging of the glucagon receptor in human. It may serve as an important tool in understanding the role of glucagon and glucagon receptor targeting drugs in metabolic disease.

REFERENCES

1. Müller TD, Finan B, Clemmensen C, DiMarchi RD, Tschöp MH. The New Biology and Pharmacology of Glucagon. *Physiol rev*. 2017;97:721-766.

2. Sánchez-Garrido MA, Brandt SJ, Clemmensen C, Müller TD, DiMarchi RD, Tschöp MH. GLP-1/glucagon receptor co-agonism for treatment of obesity. *Diabetologia*. 2017;60:1851-1861.

3. Day JW, Ottaway N, Patterson JT, et al. A new glucagon and GLP-1 co-agonist eliminates obesity in rodents. *Nat Chem Biol*. 2009;5:749-757.

4. Pocai A, Carrington PE, Adams JR, et al. Glucagon-like peptide 1/glucagon receptor dual agonism reverses obesity in mice. *Diabetes*. 2009;58:2258-66.

5. Velikyan I, Haack T, Bossart M, et al. First-in-class positron emission tomography tracer for the glucagon receptor. *EJNMMI res*. 2019;9:17.

6. Eriksson O, Irina Velikyan, Torsten Haack, et al. A Positron Emission Tomography biomarker for in vivo study of the glucagon receptor, assessed in non-human primates. *Sci rep*. 2019;9:14960.

7. Laitinen I, Jones S, Derdau V, et al. Assessment of In Vivo Glucagon Receptor Engagement in Rat Liver [abstract]. *Eur J Nucl Med Mol Imaging*. 2019;46(suppl 1):S707.

8. Evers A, Haack T, Lorenz M, et al. Design of Novel Exendin-Based Dual Glucagon-like Peptide 1 (GLP-1)/Glucagon Receptor Agonists. *J Med Chem*. 2017;60:4293-4303.

9. Elvert R, Bossart M, Herling AW, et al. Team Players or Opponents: Coadministration of Selective Glucagon and GLP-1 Receptor Agonists in Obese Diabetic Monkeys. *Endocrinology*. 2018;159:3105-3119.

10. Elvert R, Herling AW, Bossart M, et al. Running on mixed fuel-dual agonistic approach of GLP-1 and GCG receptors leads to beneficial impact on body weight and blood glucose control: A comparative study between mice and non-human primates. *Diabetes obes metab*. 2018;20:1836-1851.

11. Tillner J, Posch MG, Wagner F, et al. A novel dual glucagon-like peptide and glucagon receptor agonist SAR425899: Results of randomized, placebo-controlled first-in-human and first-in-patient trials. *Diabetes obes metab*. 2019;21:120-128.

12. Eriksson O, Haack T, Hijazi Y, et al. Receptor occupancy of dual glucagon-like peptide 1/glucagon receptor agonist SAR425899 in individuals with type 2 diabetes. *Sci rep.* 2020;x:xx. Accepted, in production.

13. Wagner M, Doverfjord JG, Tillner J, et al. Automated GMP-Compliant Production of [68Ga]Ga-DO3A-Tuna-2 for PET Microdosing Studies of the Glucagon Receptor in Humans. *Pharmaceuticals*. 2020;13:E176.

14. Velikyan I, Rosenstrom U, Eriksson O. Fully automated GMP production of [^{68}Ga]Ga-DO3A-VS-Cys40-Exendin-4 for clinical use. *Am J Nucl Med Mol Imaging*. 2017;7:111-125.

15. https://www.proteinatlas.org/ENSG00000215644-GCGR/tissue. Accessed 2020-09-21.

16. Jacobsson H, Jonas E, Hellström PM, Larsson SA. Different concentrations of various radiopharmaceuticals in the two main liver lobes: a preliminary study in clinical patients. *J Gastroenterol*. 2005;40:733–738.

FIGURES

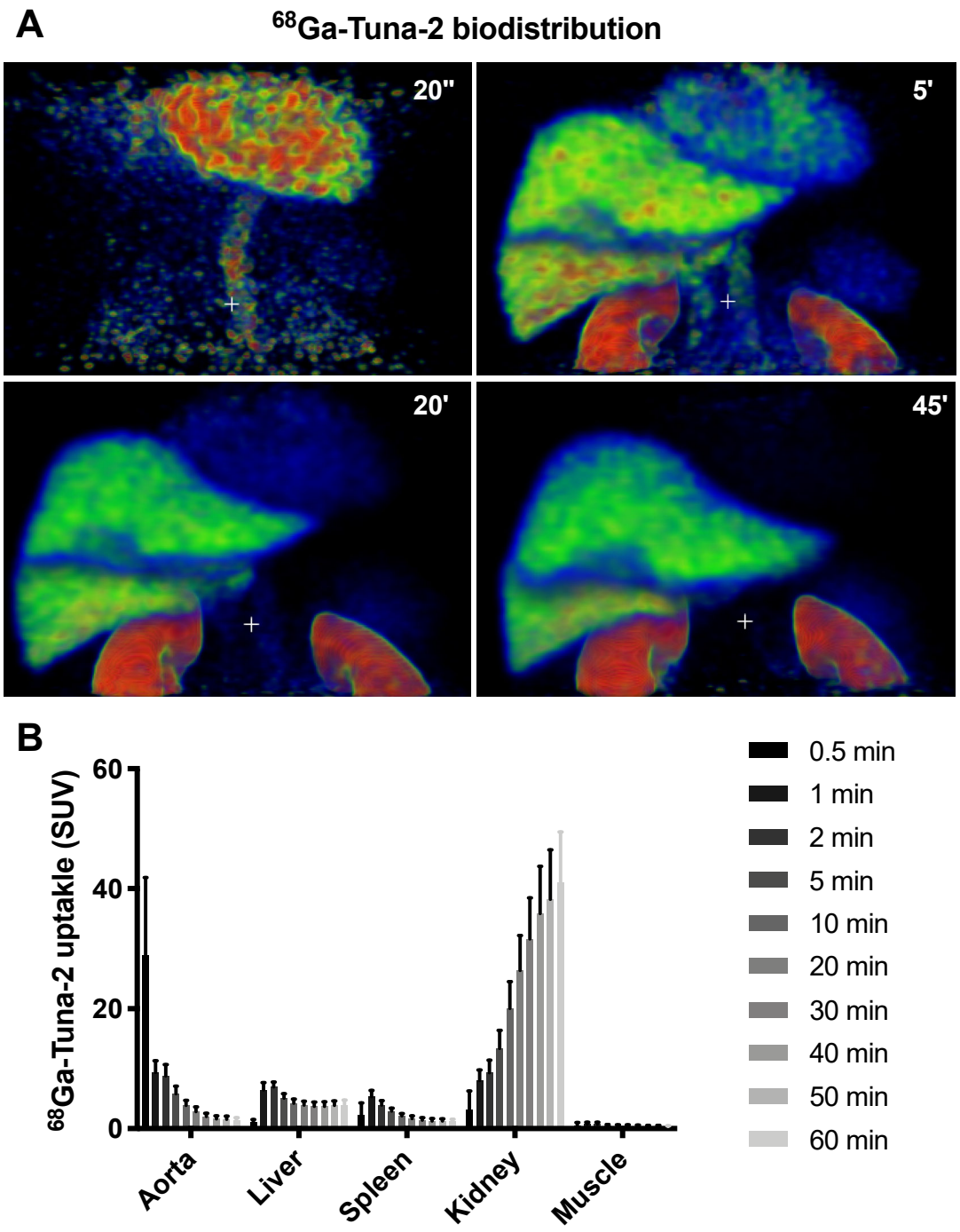

Figure 1. Representative three-dimensional projection of biodistribution in the abdominal region as assessed by PET after 20s, 5min, 20min and 45min after administration of ^{68}Ga-Tuna-2 (A). The average biodistribution (n=13 subjects diagnosed with T2D) of ^{68}Ga-Tuna-2 in abdominal tissues (B).

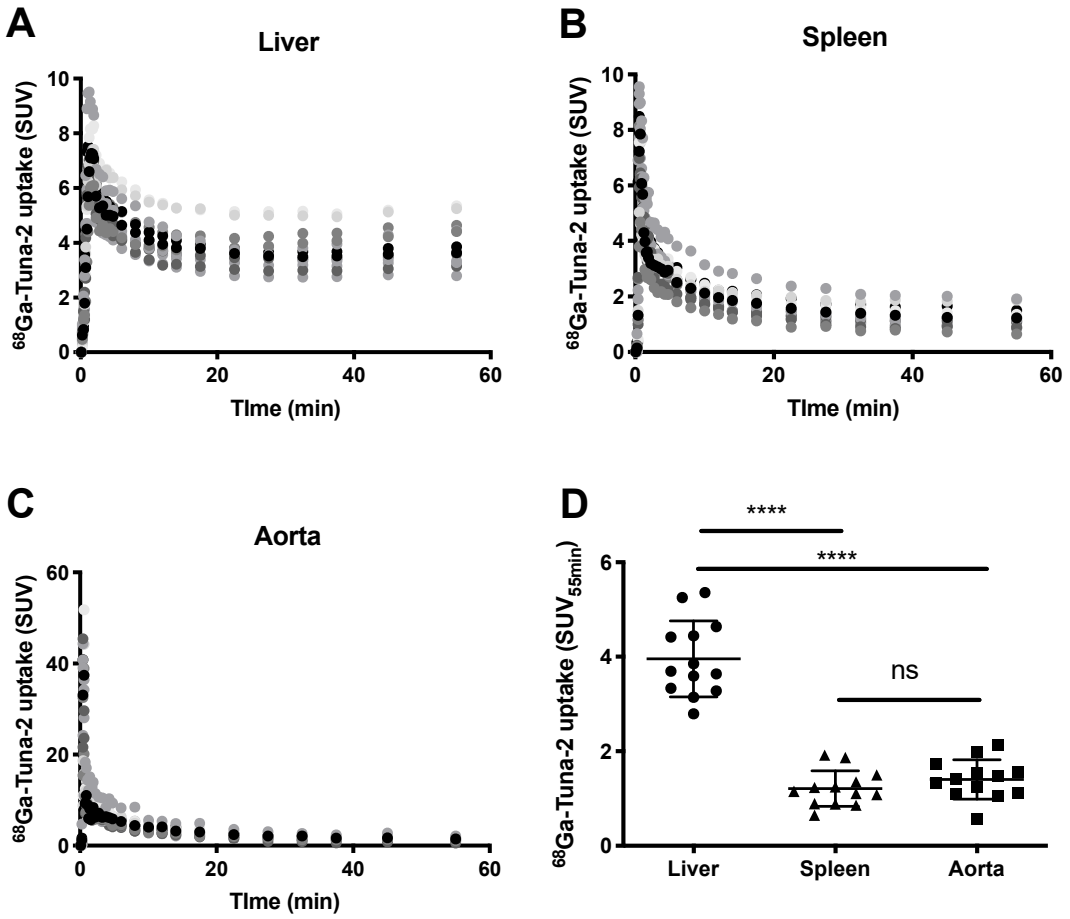

Figure 2. Dynamic uptake of ^{68}Ga-Tuna-2 in GCGR rich liver (A), GCGR negative spleen (B) and aorta (C) over 60 minutes. Comparison of uptake in the tissues at the 55min time point (SUV_{55min}, 50-60 minutes post administration) (D).

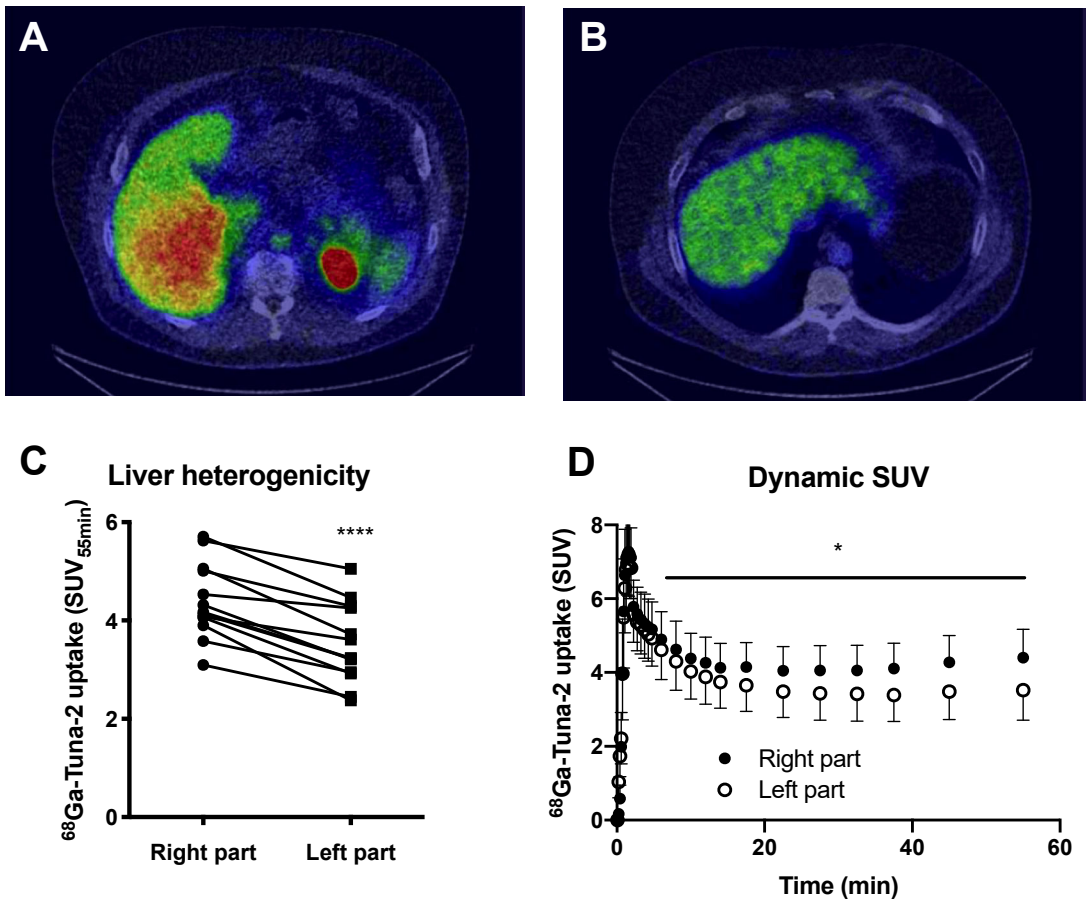

Figure 3.

Representative trans-axial images showing the distinct difference in ^{68}Ga-Tuna-2 binding in the right (A) and left (B) parts of the liver. The images are from the same time-point in the same individual, normalized to SUV 6 and thus directly comparable. The quantitatively lower GCGR density in the left part of the liver was consistent in all individuals ($p<0.001$) (C). The dynamic uptake curve in each liver part reveals that the difference increased with time after injection (D).

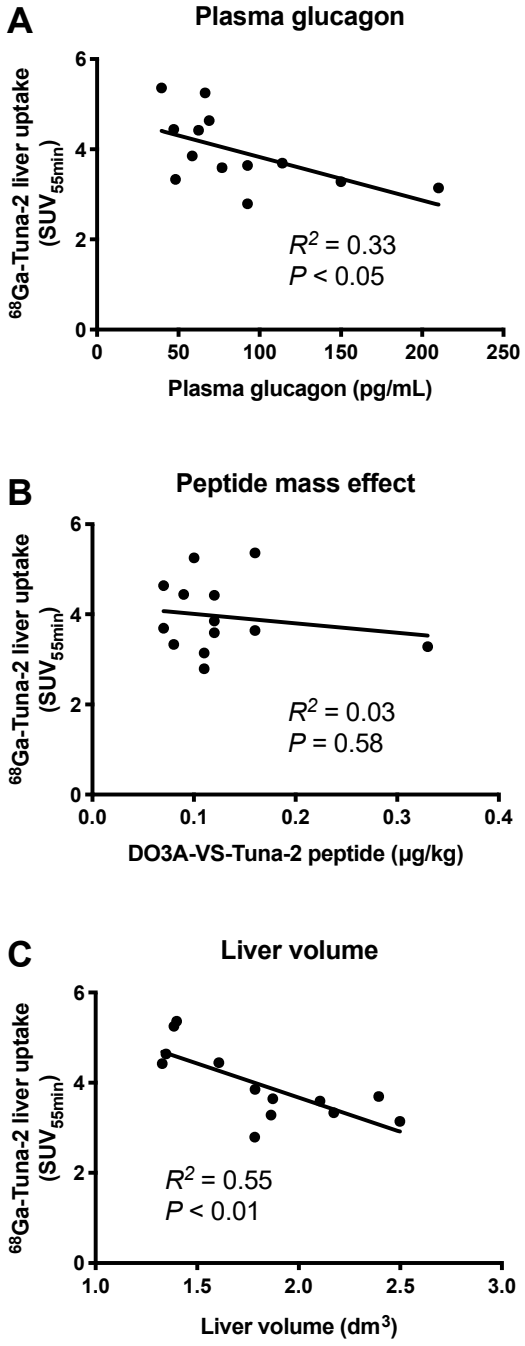

Figure 4. Correlations between liver binding (assessed as SUV_{55min}) of ^{68}Ga-Tuna-2 versus endogenous plasma glucagon levels (A), the amount of co-administered DOTA-VS-Tuna-2 peptide (B) and liver volume (C).

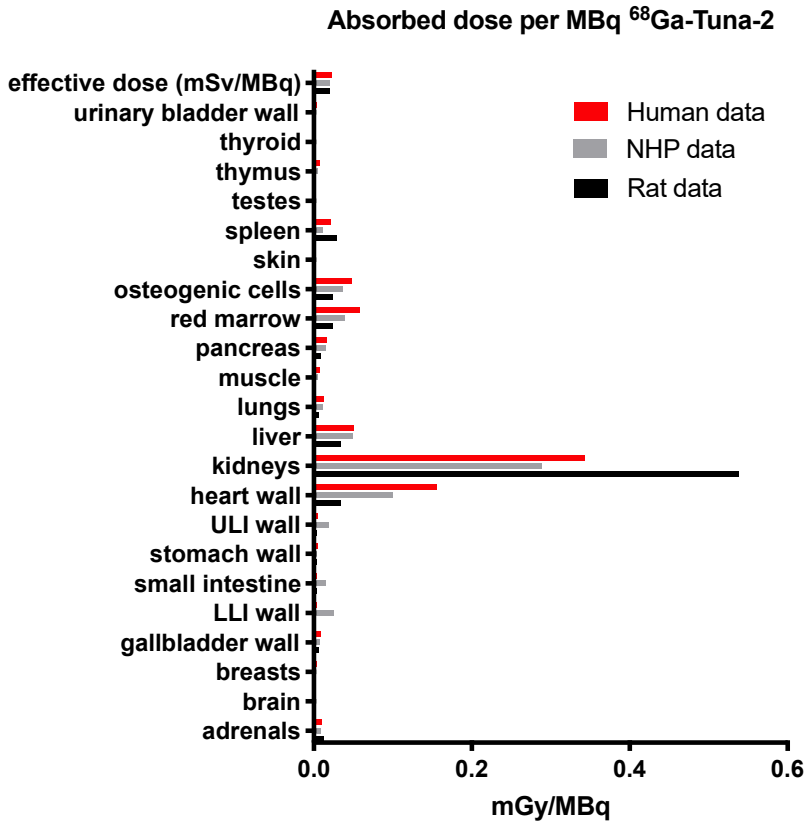

Figure 5. Human predicted dosimetry of ^{68}Ga-Tuna-2 based on human biodistribution data, compared to previously reported NHP and rat biodistribution data. ULI = Upper Large Intestine and LLI = Lower Large Intestine.

Tables

Table 1. Metabolic stability and blood plasma partition of ^{68}Ga-Tuna-2 in human (n=3).

Time (min)	Intact peptide (%)	Plasma-to-blood ratio (1/1)
5	97.8±0.6	1.85±0.04
30	92.5±0.6	1.92±0.02
60	84.3±1.6	1.91±0.03